The EMBO Journal vol.15 no.13 pp.3275–3285, 1996

Characterization of a novel component of the peroxisomal protein import apparatus using fluorescent peroxisomal proteins

Jennifer E.Kalish[1], Gilbert-Andre Keller[2], James C.Morrell[1], Stephanie J.Mihalik[3], Barbara Smith[4], James M.Cregg[4] and Stephen J.Gould[1,5,6]

Departments of [1]Biological Chemistry, [3]Pediatrics and [5]Cell Biology and Anatomy, The Johns Hopkins University School of Medicine, Baltimore, MD 21205, [2]Genentech Inc., San Francisco, CA 94080 and [4]Department of Chemistry, Biochemistry and Molecular Biology, Oregon Graduate Institute, Portland, OR 97291, USA

[6]Corresponding author

Fluorescent peroxisomal probes were developed by fusing green fluorescent protein (GFP) to the matrix peroxisomal targeting signals PTS1 and PTS2, as well as to an integral peroxisomal membrane protein (IPMP). These proteins were used to identify and characterize novel peroxisome assembly (*pas*) mutants in the yeast *Pichia pastoris*. Mutant cells lacking the *PAS10* gene mislocalized both PTS1–GFP and PTS2–GFP to the cytoplasm but did incorporate IPMP–GFP into peroxisome membranes. Similar distributions were observed for endogenous peroxisomal matrix and membrane proteins. While peroxisomes from translocation-competent *pas* mutants sediment in sucrose gradients at the density of normal peroxisomes, >98% of peroxisomes from *pas10* cells migrated to a much lower density and had an extremely low ratio of matrix: membrane protein. These data indicate that Pas10p plays an important role in protein translocation across the peroxisome membrane. Consistent with this hypothesis, we find that Pas10p is an integral protein of the peroxisome membrane. In addition, Pas10p contains a cytoplasmically-oriented C_3HC_4 zinc binding domain that is essential for its biological activity.

Keywords: green fluorescent protein/integral peroxisomal membrane protein/peroxisome assembly/protein translocation/RING finger

Introduction

Peroxisomes are ubiquitous single membrane-bound organelles that are involved in many metabolic pathways. Chief among these processes are hydrogen peroxide-based cellular respiration and fatty acid β-oxidation, while those that are more species specific include plasmalogen, bile acid and cholesterol synthesis in mammalian cells and the first two steps in methanol utilization in certain yeasts (Tolbert, 1981; Lazarow and Fujiki, 1985). The numerous and diverse pathways occurring within peroxisomes imply that this organelle is important for cellular metabolism. This inference is borne out by the observation that peroxisomes are required for normal human development. In humans, the failure to assemble normal peroxisomes results in a group of genetically heterogeneous diseases known as the peroxisome biogenesis disorders (PBDs) (Lazarow and Moser, 1995). These lethal, inherited diseases include Zellweger syndrome, neonatal adrenoleukodystrophy, infantile Refsum disease and classical rhizomelic chondrodysplasia punctata. Clinically the PBDs are characterized by severe neuronal dysfunction, mental retardation and death in early infancy. At the biochemical level, their only common feature is a defect in the import of at least one class of peroxisomal matrix proteins.

It has been proposed that peroxisomes arise from pre-existing peroxisomes and proliferate upon the selective uptake of lipids and proteins from the cytoplasm (Lazarow and Fujiki, 1985). While there is no doubt that peroxisomal proteins are transported directly from the cytoplasm to the peroxisome, there is insufficient evidence to conclude that this organelle forms from pre-existing peroxisomes. Thus, *de novo* synthesis of peroxisomes remains a formal possibility (Waterham *et al.*, 1993). Proteins destined for the peroxisome are synthesized on free polyribosomes and contain *cis*-acting peroxisomal targeting signals (PTSs) which direct them to peroxisomes (Subramani, 1993). Two PTSs have been identified for matrix proteins. Most peroxisomal matrix proteins contain PTS1, a C-terminal tripeptide consisting of the amino acids Ser–Lys–Leu (SKL) or a conservative variant (Gould *et al.*, 1987, 1988, 1989, 1990a,b; Aitchison *et al.*, 1991, 1992; Keller *et al.*, 1991; Blattner *et al.*, 1992; Didion and Roggenkamp, 1992; Distel *et al.*, 1992; Hansen *et al.*, 1992; Miura *et al.*, 1992; Swinkels *et al.*, 1992). PTS2 consists of an N-terminal segment that is ~10 residues long and has been identified in four proteins: 3-ketoacyl-CoA thiolase, watermelon malate dehydrogenase, yeast amine oxidase and *Trypanosma brucei* aldolase (Osumi *et al.*, 1991; Swinkels *et al.*, 1991; Gietl *et al.*, 1994; Glover *et al.*, 1994; Blattner *et al.*, 1995; Faber *et al.*, 1995). Both PTS1 and PTS2 appear to be involved only in directing proteins to the peroxisome lumen. Targeting signals for integral peroxisomal membrane proteins are distinct (McCammon *et al.*, 1994) but remain uncharacterized.

While PTSs direct proteins to peroxisomes, the recognition, targeting and translocation of these proteins requires a diverse set of accessory factors. To identify these factors, we and others isolated peroxisome assembly (*pas*) mutants from the yeast *Pichia pastoris* by screening for cells unable to grow on fatty acids and methanol, the utilization of which requires distinct sets of peroxisomal enzymes (Gould *et al.*, 1992; Liu *et al.*, 1992). Peroxisome assembly mutants have also been identified in the yeasts *Saccharomyces cerevisiae* (Erdmann *et al.*, 1989; Elgersma *et al.*, 1993), *Hansenula polymorpha* (Cregg *et al.*, 1990) and *Yarrowia lipolytica* (Nuttley *et al.*, 1993). Analysis of these yeast *pas* mutants, as well as studies on PBD patient fibroblasts and peroxisome-deficient Chinese hamster

ovary cell lines, has led to the identification of receptors for both PTS1 (McCollum *et al.*, 1993; van der Leij *et al.*, 1993; Dodt *et al.*, 1995; Terlecky *et al.*, 1995; Wiemer *et al.*, 1995) and PTS2 proteins (Marzioch *et al.*, 1994; Motley *et al.*, 1994; Zhang and Lazarow, 1995), as well as a host of factors required for import of peroxisomal matrix proteins. These factors include three distinct zinc-binding integral peroxisomal membrane proteins (IPMPs) (Tsukamoto *et al.*, 1991; Kalish *et al.*, 1995; Waterham *et al.*, 1996), two ATPases (Erdmann *et al.*, 1991; Spong and Subramani, 1993; Voorn-Brouwer *et al.*, 1993; Heyman *et al.*, 1994; Yahraus *et al.*, 1996), a ubiquitin-conjugating enzyme (Wiebel and Kunau, 1992; Crane *et al.*, 1994), a farnesylated protein (Kunau *et al.*, 1993; James *et al.*, 1994) and several other factors that are not members of any known protein superfamily (Höhfeld *et al.*, 1991; Kunau *et al.*, 1993; Eitzen *et al.*, 1995). In addition, the isolation and characterization of yeast *PAS* genes has led to the identification of two PBD genes, *PXR1* and *PXAAA1*, which are mutated in complementation groups 2 and 4 of the PBD cell lines, respectively (Dodt *et al.*, 1995; Yahraus *et al.*, 1996).

To identify new *pas* mutants, we developed a visual screen using a peroxisomal form of the green fluorescent protein (GFP). Wild-type cells expressing PTS1–GFP were chemically mutagenized and strains unable to import PTS1–GFP into peroxisomes were identified by fluorescence microscopy. The *P.pastoris pas10* mutant exhibited a defect in import of PTS1–GFP. We report here on the identification and characterization of the *P.pastoris PAS10* gene and its product, Pas10p. This novel protein is a zinc-binding IPMP with a C-terminal RING finger that extends into the cytoplasm. A detailed analysis of the *pas10* mutant revealed that Pas10p is essential for import of both PTS1 and PTS2 proteins into peroxisomes but is not required for targeting, inserting or orienting integral proteins into peroxisome membranes and thus for synthesis of peroxisome membranes. Furthermore, we find that most peroxisomes in *pas10* cells contain little if any peroxisomal matrix proteins and migrate to an anomalously low density in sucrose gradients. We conclude from these studies that Pas10p plays an important role in protein translocation across the peroxisome membrane.

Results

Visual screening for pas mutants using a peroxisomal form of GFP

To create a peroxisomal form of GFP, the open reading frame (ORF) of a modified GFP gene (*GFP*S65T; Helm *et al.*, 1995) was extended at its 3′-end by six codons encoding Pro-Leu-His-Ser-Lys-Leu-COOH. The C-terminal tripeptide Ser-Lys-Leu-COOH is sufficient to direct proteins to peroxisomes in all known eukaryotes (Gould *et al.*, 1989). This PTS1–GFP gene was cloned downstream of the *P.pastoris PAS8* promoter in the vector pGD79, a *HIS4*-based *P.pastoris* replicating vector (Dodt *et al.*, 1995), and introduced into *his4*Δ (wild-type) and *pas7*Δ, *his4*Δ strains of *P.pastoris*. The resultant strains were examined by fluorescence microscopy. Previously, we have shown that the *pas7*Δ strain is defective in import of PTS1 proteins (Kalish *et al.*, 1995). In wild-type cells, a punctate peroxisomal staining pattern for PTS1–GFP was observed, whereas diffuse cytoplasmic staining was detected in *pas7*Δ cells (Figure 1A and B). These results demonstrated that PTS1–GFP is an effective visual marker for peroxisomal protein import in living cells.

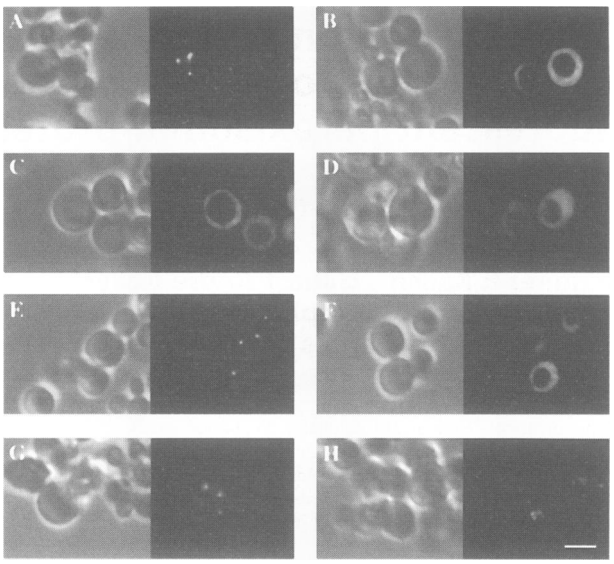

Fig. 1. Confocal fluorescence microscopy of yeast cells expressing peroxisomal forms of GFP. Phase (left panels) and fluorescence (right panels) images of (**A**) PTS1–GFP in wild-type cells, (**B**) PTS1–GFP in *pas7*Δ cells, (**C**) PTS1–GFP in *pas10-1* cells, (**D**) PTS1–GFP in *pas10*Δ cells, (**E**) PTS2–GFP in wild-type cells, (**F**) PTS2–GFP in *pas10*Δ cells, (**G**) IPMP–GFP in wild-type cells and (**H**) IPMP–GFP in *pas10*Δ cells. Bar, 5.0 μm.

Wild-type *P.pastoris* cells expressing PTS1–GFP were chemically mutagenized with *N*-methyl-*N*-nitro-*N*-nitrosoguanidine (MNNG). After a recovery period single cells were seeded on minimal dextrose medium and grown for several days. Next, each clone was examined by fluorescence microscopy to assess PTS1–GFP import, as well as for any alterations in peroxisome morphology and motility. A detailed description of the mutants derived from this screen will be presented elsewhere (S.J.Mihalik, W.-H.Lee and S.J.Gould, in preparation). The *pas10-1* strain displayed a defect in import of PTS1–GFP (Figure 1C). Furthermore, it was unable to utilize fatty acids or methanol as sole carbon source, the classic phenotype exhibited by *P.pastoris pas* mutants (Gould *et al.*, 1992).

PAS10 is required for peroxisomal import of lumenal proteins but not integral membrane proteins

The *PAS10* gene was cloned by functional complementation of the *pas10-1* mutant. Subcloning, sequencing and complementation analyses revealed that an ORF of 1230 bp was responsible for complementing activity. A strain lacking this ORF was generated by targeted gene disruption. This deletion mutant (*pas10*Δ) had the classic *pas* phenotype and was allelic to the original *pas10-1* mutant, demonstrating that we had cloned the *PAS10* gene and not a suppressor. To begin to understand the role of *PAS10* in peroxisome assembly, we compared the subcellular distribution of PTS1–GFP and two other fluorescent peroxisomal proteins, PTS2–GFP and IPMP–GFP, in wild-type and *pas10*Δ cells (Figure 1D–H). PTS1–GFP was distributed throughout the cytoplasm in *pas10*Δ cells

(Figure 1D), consistent with the phenotype of the *pas10-1* strain. Likewise, PTS2–GFP, a peroxisomal form of GFP targeted to peroxisomes via PTS2, was mislocalized to the cytoplasm in *pas10Δ* cells (Figure 1E and F), suggesting that the product of the *PAS10* gene was required for import of both classes of peroxisomal matrix proteins. In contrast, IPMP–GFP was targeted to vesicular structures in both wild-type and *pas10Δ* cells (Figure 1G and H), indicating that synthesis of peroxisome membranes and targeting of IPMPs was not dependent upon Pas10p.

To test whether the protein import phenotypes observed with these fluorescent peroxisomal marker proteins accurately reflected the protein import capabilities of *pas10Δ* cells, we examined the subcellular distribution of endogenous PTS1, PTS2 and IPMP marker proteins in wild-type and *pas10Δ* cells. These cells were incubated in oleate medium to induce peroxisome proliferation and subsequently homogenized. The post-nuclear supernatant was separated into a supernatant consisting of cytoplasm and microsomes and a pellet containing peroxisomes and mitochondria by centrifugation at 25 000 *g* (Aitchison *et al.*, 1991). Equal proportions of these two fractions were assayed for catalase, a marker for PTS1 protein import (McCollum *et al.*, 1993), thiolase, a marker for PTS2 protein import (Osumi *et al.*, 1991; Swinkels *et al.*, 1991; Glover *et al.*, 1994), and Pas7p, an IPMP (Kalish *et al.*, 1995). The majority of catalase (54% of total activity) and thiolase (72% of total protein, quantitated by densitometry) was detected in the organelle pellet of wild-type cells, as was all Pas7p (Figure 2A). In contrast, <5% of catalase activity and 15% of thiolase was detected in the organelle pellet of *pas10Δ* cells. However, Pas7p was quantitatively recovered in the 25 000 *g* pellet of *pas10Δ* cells. These data confirm that Pas10p is required for import of PTS1 and PTS2 proteins but not for targeting integral membrane proteins to peroxisomes. Essentially identical results were obtained when the post-nuclear supernatant was spun at 100 000 *g* (data not shown), demonstrating that centrifugation at 25 000 *g* quantitatively pelleted peroxisomes of *pas10Δ* cells.

The finding that Pas7p was quantitatively recovered in the 25 000 *g* pellet of *pas10Δ* cells suggested that Pas10p is not required for targeting IPMPs to peroxisomes. To determine whether Pas10p plays a role in inserting or orienting IPMPs within the peroxisome membrane, we examined the topology of Pas7p in *pas10Δ* cells. Previously, we demonstrated that Pas7p is located entirely within the peroxisome, as it is sensitive to protease only after peroxisome membranes have been disrupted with detergent (Kalish *et al.*, 1995). Organelles (25 000 *g* pellet fraction) from wild-type and *pas10Δ* cells were treated with increasing amounts of trypsin in the absence or presence of Triton X-100. Pas7p was degraded by exogenous protease only when peroxisomes from both wild-type and *pas10Δ* cells were pre-incubated with detergent (Figure 2B). The fact that Pas7p behaved identically in wild-type and *pas10Δ* cells suggests that Pas10p is not required for targeting, inserting or orienting IPMPs into the peroxisome membrane.

Multiple peroxisome populations in pas10Δ cells

Differential centrifugation and protease protection experiments suggested that Pas7p is targeted to and inserted

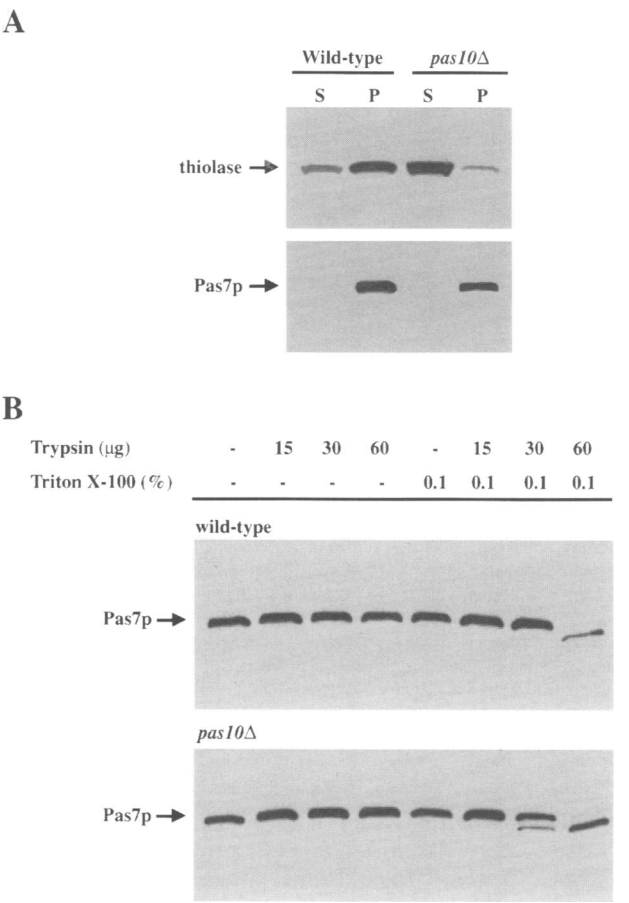

Fig. 2. The *pas10Δ* mutant is defective in import of PTS1 and PTS2 peroxisomal matrix proteins but not in targeting or insertion of peroxisomal membrane proteins. (**A**) A 25 000 *g* supernatant (S) consisting of cytosol and microsomes and a pellet (P) containing mitochondria and peroxisomes were isolated from wild-type and *pas10Δ* cells. Equal amounts of these fractions were separated by SDS–PAGE and immunoblotted with affinity-purified anti-thiolase (top panel) or anti-Pas7p antibodies (bottom panel). Antibody detection was by chemiluminescent exposure of X-ray film. (**B**) Organelles (200 μg 25 000 *g* pellets) from wild-type (top panel) and *pas10Δ* (bottom panel) strains were treated with increasing amounts of trypsin (0, 15, 30 and 60 μg) for 25 min on ice in the absence or presence of 0.1% Triton X-100. Samples (30 μg) were separated by SDS–PAGE and immunoblotted with anti-Pas7p antibodies.

into peroxisome membranes in the absence of Pas10p. However, since a 25 000 *g* pellet contains both mitochondria and peroxisomes, one remote possibility was that Pas7p had been mistargeted to mitochondria in *pas10Δ* cells. To address this possibility, organelles from a 25 000 *g* pellet of *pas10Δ* cells were separated by sucrose density gradient centrifugation. Fractions were assayed for catalase (a peroxisomal matrix enzyme marker), succinate dehydrogenase (SDH, a mitochondrial enzyme marker), density and levels of Pas7p. The clear separation between the majority of Pas7p and mitochondria in this gradient (Figure 3A) demonstrated that Pas7p is not mistargeted to mitochondria in *pas10Δ* cells.

In addition to ruling out a mitochondrial localization for Pas7p, this experiment revealed that peroxisomes of *pas10Δ* cells behaved quite differently from those of wild-type cells. Peroxisomes of wild-type cells migrate to a density of 1.21–1.23 g/cm^3 (see Figure 7B for comparison),

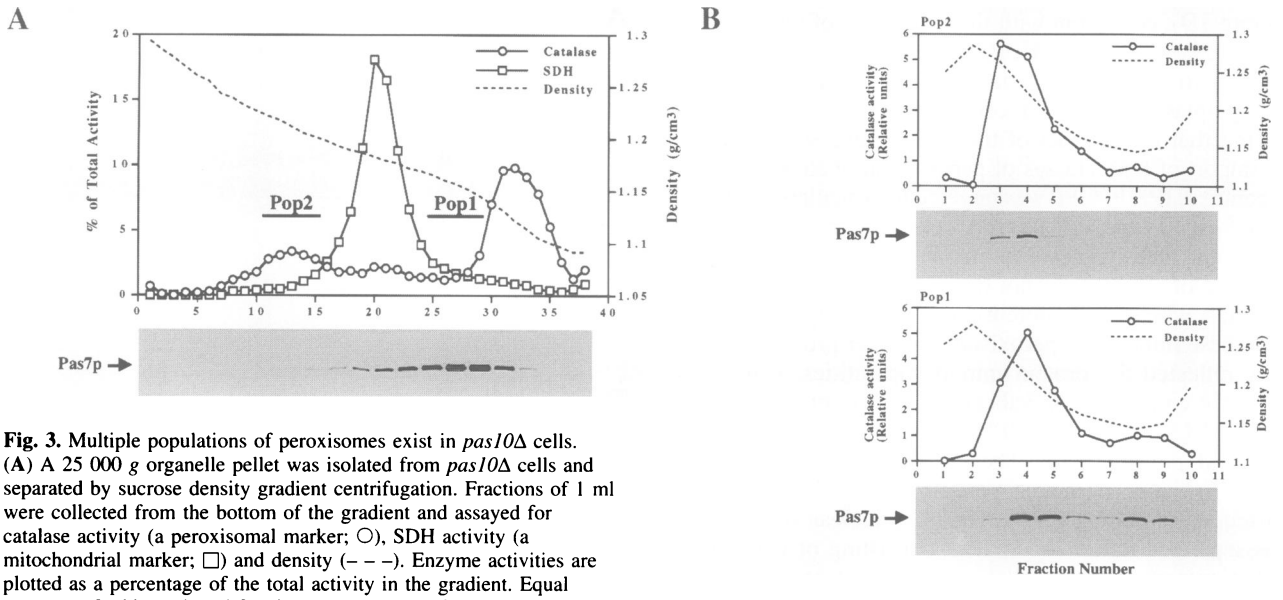

Fig. 3. Multiple populations of peroxisomes exist in *pas10Δ* cells. (**A**) A 25 000 *g* organelle pellet was isolated from *pas10Δ* cells and separated by sucrose density gradient centrifugation. Fractions of 1 ml were collected from the bottom of the gradient and assayed for catalase activity (a peroxisomal marker; ○), SDH activity (a mitochondrial marker; □) and density (– – –). Enzyme activities are plotted as a percentage of the total activity in the gradient. Equal amounts of odd numbered fractions were assayed for levels of Pas7p by immunoblot. (**B**) Five fractions that matched either the normal density catalase peak (fractions 11–15, Pop2; top panel) or the peroxisome membrane-rich peak (fractions 25–29, Pop1; bottom panel) were treated as described in Materials and methods. Ten fractions of 0.5 ml were collected from the bottom of both gradients and assayed for catalase activity (○), density (– – –) and levels of Pas7p.

whereas most peroxisomes in the *pas10Δ* mutant (assayed by detection of Pas7p) migrated to a much lower density, ~1.14–1.16 g/cm^3 (peroxisome population 1, or Pop1). Because the high protein:membrane ratio of normal peroxisomes is at least partly responsible for their high density, these data indicate that loss of Pas10p had such a severe effect on protein translocation into peroxisomes that the density of the organelle was lowered significantly. However, a small subset of peroxisomes in *pas10Δ* cells (<2%) did sediment at the high density typical of normal peroxisomes (Pop2; compare with the gradient of wild-type cells in Figure 7B). These few peroxisomes contained almost as much catalase activity as all other peroxisomes of *pas10Δ* cells.

To further investigate the distribution of Pas7p and catalase in these two peroxisome populations of *pas10Δ* cells, we performed two-step flotation gradient analysis (Heyman *et al.*, 1994). This procedure differentiates between membrane-associated proteins, which migrate into the gradient, and protein aggregates, which remain at the bottom of the gradient. An organelle pellet from *pas10Δ* cells was fractionated by sucrose density centrifugation. Five fractions that matched the densities of Pop1 and Pop2 were each pooled, overlaid with 60 and 28% sucrose and spun at 170 000 *g* for 18 h. Ten fractions of 0.5 ml were collected from the bottom of each flotation gradient and assayed for catalase activity, density and levels of Pas7p by Western blot analysis (Figure 3B). Catalase and Pas7p were detected at or above the 60/28% sucrose interface in both gradients, indicating that these proteins were organelle associated. Furthermore, the low density peroxisome population was resolved into light and heavy components, Pop1L and Pop1H. Quantitation of catalase and Pas7p levels allowed us to calculate relative ratios for these matrix and membrane protein markers. Pop1L had a relative catalase:Pas7p ratio of 1, Pop1H displayed a ratio of 2 and Pop2 exhibited a ratio of 24. These data suggest that *pas10Δ* cells contain multiple peroxisome populations which are distinguishable by differences in their relative matrix protein content. Furthermore, the low matrix:membrane protein ratios for most peroxisomes of *pas10Δ* cells are what one would expect if peroxisomes exhibited a severely reduced rate of protein translocation across the membrane.

Electron microscopic analysis of the pas10Δ mutant

The gradations of matrix protein content observed for peroxisomes of oleate-induced *pas10Δ* cells should also be reflected in their morphologies. Wild-type and *pas10Δ* cells were incubated in either methanol or oleic acid medium and processed for electron microscopy. We observed large attached peroxisomes in wild-type cells incubated in methanol medium (Figure 4A), whereas oleate-grown cells contained smaller spherical peroxisomes that were dispersed throughout the cell (Figure 4B). These carbon source-specific peroxisome morphologies have been noted previously in *P.pastoris* and can be useful to identify peroxisomes (Gould *et al.*, 1992; Kalish *et al.*, 1995). In contrast to the peroxisomes of wild-type cells, peroxisomes of *pas10Δ* cells incubated in methanol appeared as clusters of attached oblong structures (Figure 4C and E), while oleate-induced *pas10Δ* cells contained small unattached peroxisomes encompassing little matrix space (Figure 4D and F). Furthermore, the peroxisomes of oleate-induced *pas10Δ* cells spanned a wide variety of morphologies, varying from dumbbell-shaped structures with barely any lumenal space to more spherical structures that appeared to contain more matrix content. The identification of these structures as peroxisomes can be inferred since they were never observed in wild-type cells and

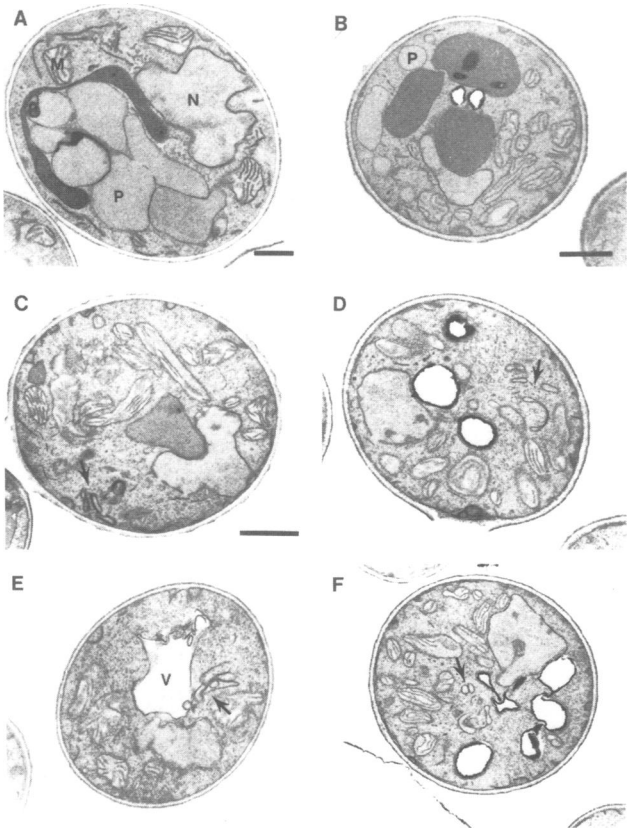

Fig. 4. Peroxisomes of several morphologies are observed in *pas10Δ* cells. Wild-type (**A** and **B**) and *pas10Δ* (**C–F**) cells were incubated in methanol (A, C and E) or oleic acid medium (B, D and F) for 18 h and processed for transmission electron microscopy. P, peroxisome; M, mitochondria; N, nucleus; V, vacuole. The arrows point to peroxisomes of *pas10Δ* cells. (A) and (E), (B) and (D) and (C) and (F) are of the same magnification. Bar, 1.0 μm.

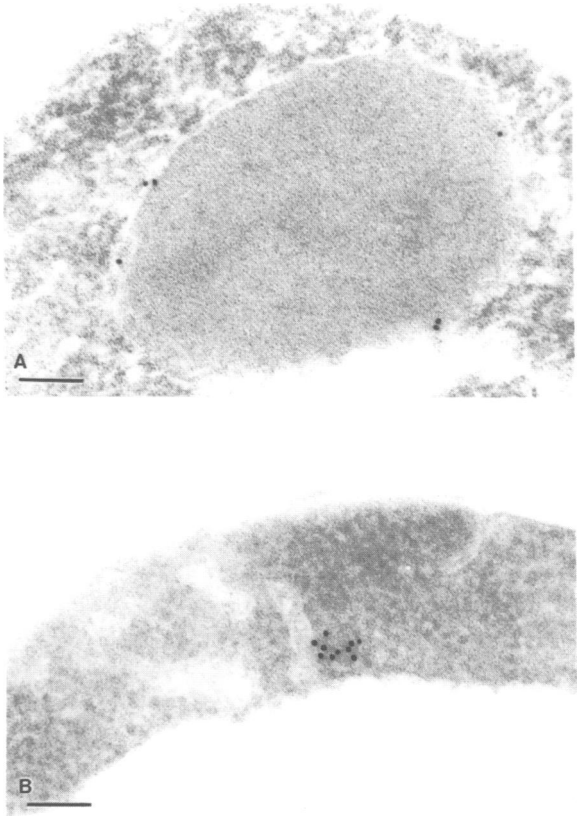

Fig. 5. Immunoelectron microscopic detection of peroxisomes in wild-type and *pas10Δ* cells. Wild-type (**A**) and *pas10Δ* (**B**) cells were incubated in methanol medium for 18 h and processed for immunoelectron microscopy with antibodies specific for the IPMP and Pas7p and subsequently detected using protein A–gold particle (10 nm) conjugates. Bar, 0.1 μm.

were specifically induced by incubation in methanol and fatty acid media.

We also tested whether peroxisomes of *pas10Δ* cells could be detected by immunoelectron microscopy using antibodies specific for Pas7p (Figure 5), an integral protein of the peroxisome membrane (Kalish *et al.*, 1995). As expected, the anti-Pas7p antibodies decorated the peroxisome membrane of wild-type cells. These antibodies also stained the inside of small vesicles in *pas10Δ* cells that were similar in size and shape to the peroxisomes of *pas10Δ* cells observed by transmission electron microscopy. Protease protection experiments have demonstrated that Pas7p is entirely protected from external protease in both wild-type and *pas10Δ* cells and the gold particle labeling in these immunoelectron microscopy images is consistent with this topology.

PAS10 encodes an integral peroxisomal membrane protein

Examination of the deduced amino acid sequence of Pas10p (Figure 6) revealed two putative membrane spanning segments (amino acids 171–195 and 266–282), suggesting that Pas10p might be an integral membrane protein. To determine its subcellular location, we first generated affinity-purified polyclonal antibodies against the C-terminal 120 amino acids of Pas10p. Immunoblot analysis demonstrated that these antibodies were specific for Pas10p, detecting a single 46 kDa band in wild-type cells which was absent in the *pas10Δ* mutant (data not shown). Next, a post-nuclear supernatant from wild-type cells was separated into a supernatant consisting of cytosol and microsomes and a pellet containing mitochondria and peroxisomes by centrifugation at 25 000 *g*. Pas10p was detected solely in the pellet when equal proportions of these fractions were analyzed by immunoblot (Figure 7A). Mitochondria and peroxisomes in this pellet were next separated by sucrose density centrifugation and Pas10p co-localized with the peroxisomal matrix protein catalase (Figure 7B), as well as with other peroxisomal proteins (data not shown). Furthermore, Pas10p remained associated with the membrane during hypotonic lysis of organelles and extraction of organelle membranes with 100 mM Na_2CO_3, pH 11.5, a treatment that strips all but integral proteins from membranes (Figure 7C). Thus, biochemical techniques indicate that Pas10p, is an IPMP.

To determine the topology of Pas10p, a protease protection assay was performed (as described in Figure 2B). Pas10p was trypsin accessible even in the absence of detergent (Figure 7D, top panel), indicating that its C-terminus extends into the cytoplasm (the antibodies were specific for the C-terminal 120 amino acids of Pas10p, the region downstream of the second putative transmembrane domain). In contrast, the soluble lumenal protein thiolase was degraded by trypsin only when

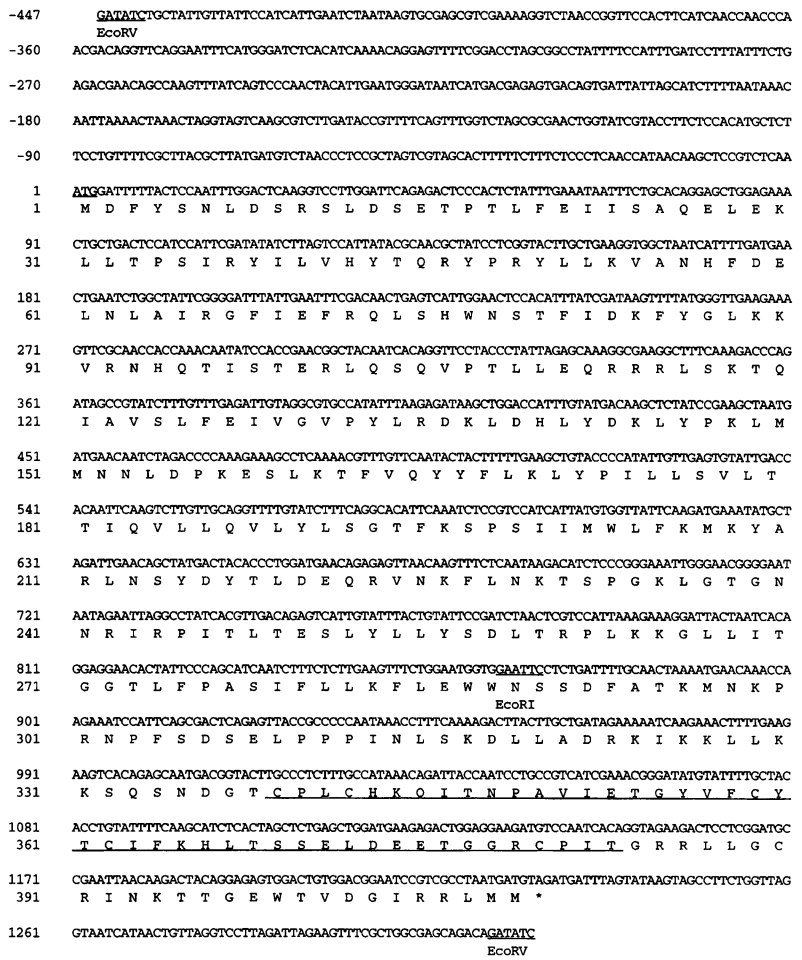

Fig. 6. Nucleotide sequence of *PAS10* and its deduced amino acid sequence. The nucleotide sequence of a 1765 bp *Eco*RV fragment that encompasses the *PAS10* gene was determined in its entirety on both strands. The start codon, relevant restriction enzyme sites and the C_3HC_4 zinc-binding motif are underlined. The stop codon is highlighted with an asterisk. The deduced amino acid sequence is presented as single letter code. These sequence data are available from EMBL/GenBank/DDBJ databases under accession No. U58140.

organelle membranes were disrupted with detergent (Figure 7D, bottom panel).

The C-terminal zinc RING finger motif of Pas10p is essential for its biological activity

Pas10p contains a putative C_3HC_4 zinc-binding domain within its C-terminal 70 amino acids (Freemont *et al.*, 1991). Although only five of the eight consensus zinc-binding residues exist in the C_3HC_4 domain of Pas10p, all other conserved hydrophobic amino acids of the RING finger motif are present (Figure 8A). Three-dimensional structures of C_3HC_4 zinc-binding domains have been solved, revealing that RING fingers bind two zinc ions via clusters of cysteine and histidine residues (Barlow *et al.*, 1994; Borden *et al.*, 1995). If each of the eight zinc binding residues is designated by a roman numeral and ordered in the direction of the polypeptide chain, the first zinc ion is coordinated by residues I, II, V and VI (all Cys), while the second ion is bound by Cys III, His IV and Cys VII and VIII. Applying this structural model to Pas10p, it appeared that Pas10p contained all necessary residues for the first zinc binding site but lacked three of the four residues predicted to coordinate the second zinc ion. Thus Pas10p may bind only one zinc ion.

To determine whether this putative zinc-binding domain was important for biological activity of Pas10p, a series of mutations were created and assayed for their ability to rescue the methanol growth defect of the *pas10Δ* mutant. Deletion of either the entire RING domain (ΔC120) or the region downstream of Cys VI (ΔC41) completely abolished Pas10p activity (data not shown). Loss of *PAS10* function was also observed when we substituted serine for either of two pairs of cysteine residues (C339S and C359S or C339S and C362S) predicted to play a direct role in binding zinc ions (Figure 8B).

Because the RING finger of Pas10p was essential for biological activity of this protein, we next examined whether it could physically bind zinc ions. The C_3HC_4 domain of Pas10p (encompassed within the 120 C-terminal amino acids) was expressed in *Escherichia coli* as a maltose binding protein (MBP) fusion, purified and analyzed by atomic absorption spectroscopy. The observed molar ratio of zinc to protein for purified MBP–Pas10p was ~0.3. Although 0.3 is less than the predicted value of one zinc ion per Pas10p molecule, neither MBP alone nor a control fusion protein, MBP–Pxr1p (Kalish *et al.*, 1995), bound any zinc (depressed zinc-binding capacities for bacterially synthesized zinc-binding proteins have been noted; Borden *et al.*, 1995). When MBP–Pas10p was dialyzed overnight against 1 mM EDTA and re-assayed

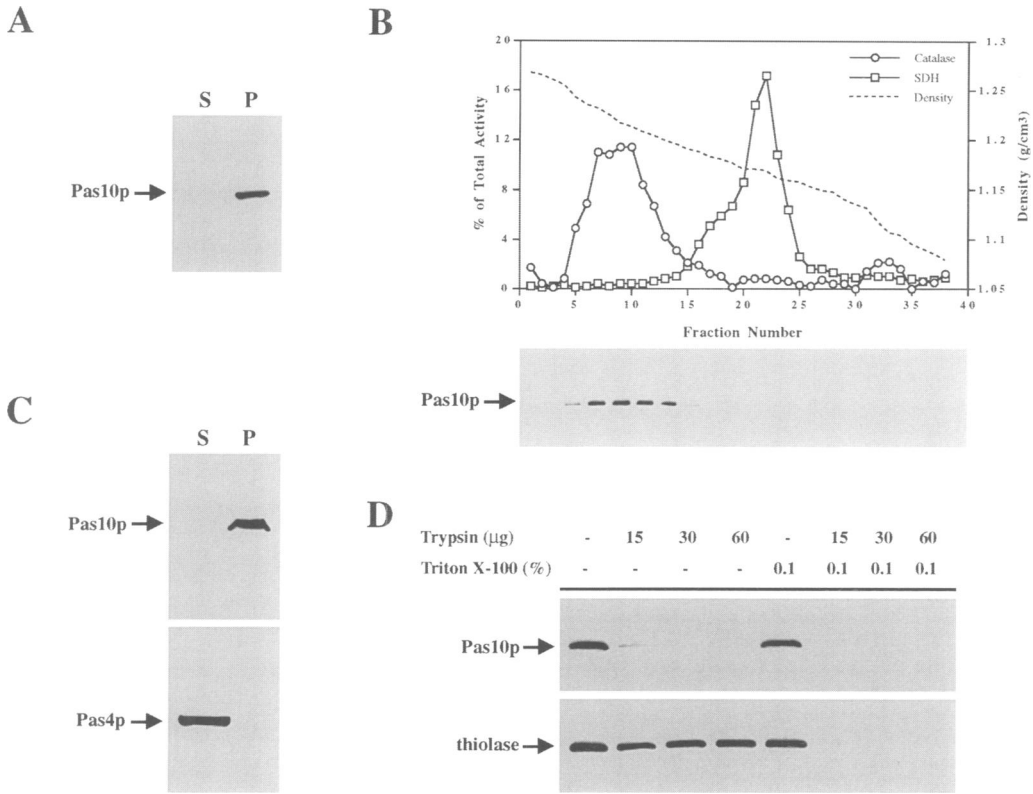

Fig. 7. Pas10p is an IPMP with its C-terminus extending into the cytoplasm. (**A**) Equal proportions of 25 000 *g* supernatant (S) and pellet (P) fractions from wild-type yeast cells were analyzed by immunoblot with affinity-purified anti-Pas10p antibodies. (**B**) Mitochondria and peroxisomes were fractionated as described in Figure 3A. Equal amounts of odd numbered fractions were assayed for levels of Pas10p by immunoblot. (**C**) A membranous pellet was resuspended in 100 mM Na_2CO_3, pH 11.5, incubated on ice for 30 min and spun at 200 000 *g* for 30 min. A supernatant (S) consisting of peripheral membrane proteins and a pellet (P) containing integral membrane proteins were analyzed by immunoblot with anti-Pas10p (top panel) and anti-Pas4p (bottom panel) antibodies. Pas4p is a peripheral peroxisomal membrane protein (Crane *et al.*, 1994). (**D**) Protease protection assays were performed as described in Figure 2B. Anti-Pas10p (top panel) and anti-thiolase (bottom panel) antibodies were utilized for immunoblot analysis.

for the amount of zinc bound, the molar ratio of 0.3 was unchanged, demonstrating that zinc was tightly bound to this fusion protein.

Discussion

We have demonstrated the utility of peroxisomal forms of GFP for the isolation and characterization of novel *pas* mutants defective in peroxisomal protein import. More importantly, these studies led to the identification of *P.pastoris PAS10* and characterization of its product, Pas10p. This protein is an IPMP that contains a C-terminal RING finger which is essential for its biological activity. Furthermore, biochemical and ultrastructural analysis of the *pas10Δ* mutant suggests that Pas10p is involved in protein translocation across the peroxisome membrane.

Pas10p plays a specific role in matrix protein import

The role of Pas10p in peroxisome assembly was addressed by examining the import capabilities of peroxisomes depleted of this protein. Fluorescence microscopy analysis of *pas10Δ* cells expressing either PTS1–GFP, PTS2–GFP or IPMP–GFP demonstrated that Pas10p is required for import of PTS1 and PTS2 proteins but is dispensable for targeting an integral membrane protein to peroxisomes. Traditional biochemical analyses of *pas10Δ* cells led to the same conclusion. In addition, protease protection experiments and immunoelectron microscopy studies revealed that the endogenous IPMP Pas7p (Kalish *et al.*, 1995) had inserted and oriented properly into the peroxisome membrane of *pas10Δ* cells. Although the total membrane surface area of peroxisomes is much lower in *pas10Δ* cells than in wild-type cells, similar levels of Pas7p were detected in organelle pellet fractions from both strains. Consistent with this observation, antibodies specific for Pas7p appeared to label the peroxisome membrane more densely in *pas10Δ* cells than in wild-type cells. Taken together, these studies indicate that Pas10p is required for import of peroxisomal matrix proteins but is not required for targeting, inserting or orienting IPMPs into peroxisome membranes and thus for synthesis of peroxisome membranes.

Pas10p is involved in peroxisomal protein translocation

While the data clearly show that Pas10p is required for import of peroxisomal matrix proteins, what is its role in the import process? One approach used to address the function of a peroxisome assembly factor is to examine the properties of peroxisomes in the corresponding *pas* mutant. For instance, peroxisomes of *P.pastoris pas1* and *pas5* cells import sufficient amounts of peroxisomal matrix proteins to sediment in sucrose gradients at the density

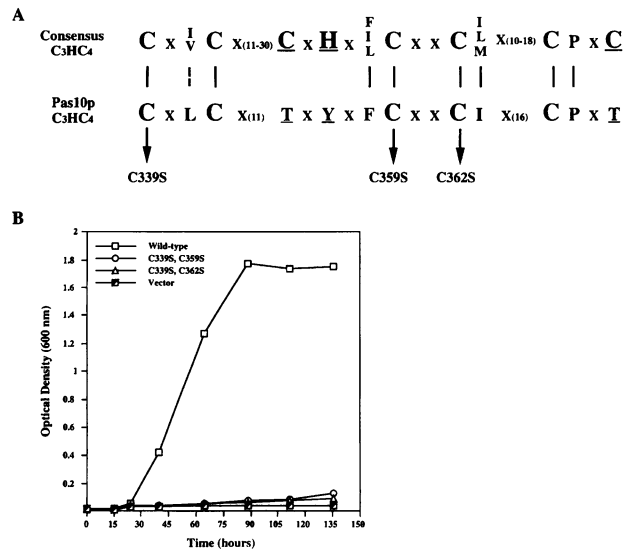

Fig. 8. The RING finger of Pas10p is essential for its biological activity. (**A**) Comparison of the consensus C_3HC_4 zinc-binding motif and the RING finger of Pas10p. Conserved residues of the C_3HC_4 motif are represented by one letter code and X denotes non-conserved positions. Solid lines represent amino acid identities, the dashed line denotes an amino acid similarity and underlined residues show deviations from the conserved C_3HC_4 motif. (**B**) *HIS4*-based replicating vectors containing either wild-type *PAS10*, double point mutants (C339S, C359S or C339S, C362S) or no insert (vector) were transformed into the *pas10Δ*, *his4Δ* strain. HIS^+ transformants were selected on minimal dextrose medium and tested for growth in liquid methanol medium. Optical densities of the cultures were measured at 600 nm over a period of 135 h.

typical of peroxisomes (Spong and Subramani, 1993; Heyman *et al.*, 1994). Based on these findings, Heyman *et al.* (1994) and Spong and Subramani (1993) concluded that Pas1p and Pas5p are not involved in protein translocation across the peroxisome membrane. In contrast, subcellular fractionation and ultrastructural analyses revealed that the vast majority of peroxisomes (98%) of *pas10Δ* cells migrated to an anomalously low density in sucrose gradients and appeared to contain little lumenal space. Thus, peroxisome membranes form in the absence of Pas10p, but translocation of proteins across these membranes may be extremely inefficient.

Defects in the import of PTS1 and PTS2 proteins have also been reported for other yeast *pas* mutants and human PBD cell lines. For example, *P.pastoris pas7* cells (Kalish *et al.*, 1995) display a similar yet more severe defect in protein translocation than *pas10Δ* cells. PBD fibroblasts from complementation groups 3 and 10 also appear to be unable to import peroxisomal matrix proteins (Slawecki *et al.*, 1995). However, the majority of *pas* mutants are translocation competent, importing small amounts of both PTS1 and PTS2 proteins into peroxisomes. This phenotype has been observed for *P.pastoris pas1*, *pas5* and *pas4* mutants (Spong and Subramani, 1993; Heyman *et al.*, 1994; J.E.Kalish and S.J.Gould, in preparation) and PBD fibroblasts from complementation groups 1, 4, 6 and 8 (Slawecki *et al.*, 1995). Recently, the gene mutated in PBD group 4 cells, *PXAAA1*, was identified and shown to be the human ortholog of *P.pastoris PAS5* (Yahraus *et al.*, 1996). A selective defect in PTS1 or PTS2 protein import has been reported for cells carrying mutations in the PTS1 and PTS2 receptor genes (McCollum *et al.*, 1993; van der Leij, 1993; Marzioch *et al.*, 1994; Dodt *et al.*, 1995; Zhang and Lazarow, 1995). In addition, a more generalized peroxisome assembly defect, characterized by an inability to import peroxisomal membrane proteins, as well as PTS1 and PTS2 matrix proteins, has been observed in a yeast mutant (Waterham *et al.*, 1993) and a PBD fibroblast cell line (G.Dodt and S.J.Gould, manuscript submitted). These phenotypes suggest the existence of at least one gene involved either in the synthesis of peroxisome membranes or targeting IPMPs to the peroxisome membrane.

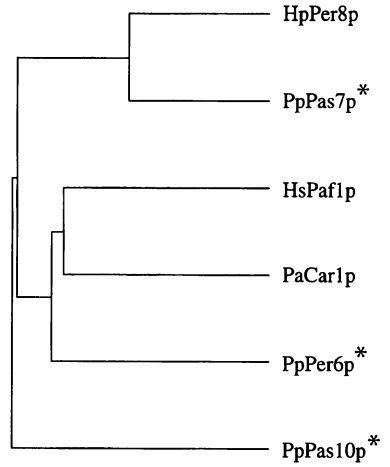

Fig. 9. Dendogram representation of relatedness between known zinc binding peroxisome assembly factors. Sequences of all six proteins were analyzed using the PILE-UP algorithm of the GCG package with a gap width of 3.0 and gap extension of 0.1. Branch lengths are a measure of divergence among the proteins. Abbreviations: Hp, *H.polymorpha*; Hs, *Homo sapiens*; Pa, *P.anserina*; Pp, *P.pastoris*.

Pas10p represents the third zinc-binding IPMP required for peroxisome assembly

Pas10p is an IPMP required for peroxisome assembly and a C_3HC_4 zinc-binding protein. These properties have been found in two other *P.pastoris* proteins, Pas7p (Kalish *et al.*, 1995) and Per6p (Waterham *et al.*, 1996), as well as in human Paf1p, *H.polymorpha* Per8p (Tan *et al.*, 1995) and *Podospora anserina* Car1p (Berteaux-Lecellier, 1995). We examined the amino acid sequences of these six proteins using the relatedness algorithm PILE-UP (Genetics Computer Group Inc., Madison, WI). The results of this analysis are presented as a dendogram in which the branch lengths are a relative measure of divergence (Figure 9). Pas10p appears to be a unique peroxisome assembly factor, whereas *P.pastoris* Pas7p and *H.polymorpha* Per8p represent a second subfamily and *P.pastoris* Per6p is most closely related to human Paf1p and *P.anserina* Car1p. Given that *P.pastoris* Pas10p, Pas7p and Per6p all share similar general features, it will be particularly interesting to determine whether there is any functional redundancy between these proteins. Such redundancy would most likely occur for Pas10p and Per6p because their RING fingers both extend into the cytoplasm.

The zinc-binding domain of Pas10p is essential for biological activity

Unlike other members of the RING finger superfamily, Pas10p does not contain all eight zinc-binding residues of

Table I. Yeast strains and their source or reference

Strain	Genotype	Source/reference
PPY3	*arg4-1*	Gould *et al.* (1992)
SGY30	*arg4-1*, *his4Δ::ARG4* (pSM102)	this study
SGY31	*arg4-1*, *his4Δ::ARG4* (pJM205)	this study
SGY32	*arg4-1*, *his4Δ::ARG4* (pJM182)	this study
SGY55	*arg4-1*, *his4Δ::ARG4*	Crane and Gould (1994)
SGY132	*arg4-1*, *pas7Δ::LEU2*, *his4Δ::ARG4*	Kalish *et al.* (1995)
SGY48	*arg4-1*, *pas7Δ::LEU2*, *his4Δ::ARG4* (pSM102)	this study
SGY400A	*arg4-1*, *pas10-1*	this study
SGY400	*arg4-1*, *pas10-1*, *his4Δ::ARG4*	this study
SGY431	*arg4-1*, *pas10Δ::ARG4*, *his4Δ::ARG4* (pJEK70)	this study
SGY435	*arg4-1*, *pas10Δ::ARG4*, *his4Δ::ARG4* (pJEK72)	this study
SGY438	*arg4-1*, *pas10Δ::ARG4*, *his4Δ::ARG4* (pJM50.1)	this study
SGY439	*arg4-1*, *pas10Δ::ARG4*, *his4Δ::ARG4* (pSG927)	this study
SGY443	*arg4-1*, *pas10Δ::ARG4*, *his4Δ::ARG4*	this study
SGY456	*arg4-1*, *pas10Δ::ARG4*, *his4Δ::ARG4* (pJEK107)	this study
SGY459	*arg4-1*, *pas10Δ::ARG4*, *his4Δ::ARG4* (pJEK127)	this study
SGY60	*arg4-1*, *pas10-1*, *his4Δ::ARG4* (pSM102)	this study
SGY68	*arg4-1*, *pas10Δ::ARG4*, *his4Δ::ARG4* (pSM102)	this study
SGY69	*arg4-1*, *pas10Δ::ARG4*, *his4Δ::ARG4* (pJM205)	this study
SGY70	*arg4-1*, *pas10Δ::ARG4*, *his4Δ::ARG4* (pJM182)	this study

the classical C_3HC_4 motif but only enough to form a single zinc-binding cluster (Freemont *et al.*, 1991; Barlow *et al.*, 1994; Borden *et al.*, 1995). Nevertheless, substituting Ser for either of two pairs of zinc-binding Cys residues eliminated Pas10p activity, as did deletion of the entire zinc-binding domain or its C-terminal half. Furthermore, a bacterially synthesized protein that contains the putative zinc-binding domain of Pas10p did bind zinc ions. Taken together these data suggest that Pas10p is a zinc binding protein and that zinc binding is required for its function. It will be interesting to determine whether this domain is merely required for Pas10p to attain its proper tertiary structure in the peroxisome membrane or whether Pas10p uses this zinc-binding domain to interact with other components of the peroxisomal protein import machinery. Given the importance of Pas10p for protein translocation into the peroxisome lumen, characterization of its zinc-binding domain may aid in identifying other proteins involved in import.

Materials and methods

Strains

The *P.pastoris* strains utilized in this report are shown in Table I and were grown as described (Gould *et al.*, 1992). The *E.coli* strain DH10B was used for all bacterial manipulations (Grant *et al.*, 1990).

Plasmid construction

All cloning and subcloning procedures were carried out as described in Sambrook *et al.* (1989). Peroxisomal forms of GFP were constructed using the S65T-*GFP* mutant (Helm *et al.*, 1995). PTS1–GFP was created by PCR mutagenesis, directly appending the sequence 5′-CCACTGCACTCAAAACTC-3′ immediately upstream of the stop codon. PTS2–GFP and IPMP–GFP were also created by PCR, appending the *GFP*-S65T ORF to the 3′-end of the *S.cerevisiae* thiolase ORF (Igual *et al.*, 1991) and the *PXSH3* ORF (Gould *et al.*, 1996) respectively. Human *PXSH3* encodes a 43 kDa IPMP. Each peroxisomal GFP gene was originally constructed in the vector pcDNA3 (Invitrogen). For expression in yeast, modified GFP genes were cloned downstream of the *PAS8* promoter in the vector pGD79 (Dodt *et al.*, 1995), creating pSM102 (PTS1–GFP), pJM205 (PTS2–GFP) and pJM182 (IPMP–GFP).

The *PAS10* gene was cloned by functional complementation of the *pas10-1* strain using a *HIS4*-based *P.pastoris* genomic DNA library. Full complementing activity was found within a 1765 base pair (bp) *Eco*RV fragment. pJM50.1 consisted of this *Eco*RV fragment in the *Eco*RV site of the *HIS4*-based replicating plasmid pSG927 (Crane and Gould, 1994). The plasmid (pJM66) utilized for chromosomal deletion of the *PAS10* gene was created by inserting 425 nucleotides of the 5′-untranslated region of *PAS10* and 440 nucleotides of the 3′-untranslated region of *PAS10* upstream and downstream of the *S.cerevisiae ARG4* gene respectively in the plasmid pSG915. Truncations at the 3′-end of the *PAS10* gene were generated by removing either the C-terminal 120 codons (ΔC120, pJEK70) or the C-terminal 41 codons (ΔC41, pJEK72). The Cys→Ser substitution mutants were created by site-directed mutagenesis using the C339S oligonucleotide (5′-GACGGTACCTCCCCT-CTTTGCCATAAACAG-3′) and either the C359S oligonucleotide (5′-AGAACTAGTGAGATGCTTGAAAATACAGGTGTAGGAAAATAC-ATA-3′) or the C362S oligonucleotide (5′-AGAACTAGTGAGATGCT-TGAAAATAGAGGTGTAGCA-3′). Structures of the *PAS10–C339S*, *C359S* (pJEK107) and *PAS10–C339S*, *C362S* (pJEK127) genes were confirmed by restriction mapping and sequence analysis (Sanger *et al.*, 1977). The plasmid (pJM59) used for expression of the C-terminal 120 amino acids of Pas10p in bacteria (for generation of antibodies and zinc-binding studies) was created by inserting the 462 bp *Eco*RI fragment from pJM50.1 into the *Eco*RI site of pMAL-c2 (New England Biolabs). The vector (pJEK21) used for expression of thiolase in *E.coli* was constructed by inserting the *S.cerevisiae* thiolase ORF between the *Bam*HI and *Xba*I sites of pMAL-c2.

DNA recovery from yeast and yeast transformations

DNA was extracted from yeast cells according to a modified protocol of Hoffman and Winston (1987), as outlined previously (Crane *et al.*, 1994). Isolated DNA was amplified in *E.coli* and reintroduced into yeast strains by electroporation (Cregg *et al.*, 1985; Crane *et al.*, 1994). The *pas10* disruption strain (*pas10Δ*) was generated by transformation of the linear Asp718–*Spe*I fragment of pJM66 into PPY3 and selecting for ARG^+ prototrophs. The desired rearrangement was confirmed by Southern blot analysis.

Fluorescence, electron and immunoelectron microscopy

Yeast cells expressing peroxisomal forms of GFP were examined with a Bio-Rad MRC-600 scanning laser confocal imaging system. For both electron and immunoelectron microscopy studies, wild-type (SGY55) and *pas10Δ* (SGY443) cells were grown in dextrose medium and then incubated in methanol or oleic acid medium for 18 h to induce peroxisome proliferation. Transmission electron microscopy was performed as described previously (Gould *et al.*, 1992). For immunoelectron microscopy cells were fixed with 0.5% glutaraldehyde, 3% formaldehyde, 0.2 M cacodylate buffer, pH 7.2, on ice overnight and processed as described (Keller *et al.*, 1987). Labeling was performed with protein A–gold conjugates (10 nm).

Quantitation of zinc in protein samples

The plasmid pJM59, containing the C_3HC_4 domain of Pas10p, was introduced into DH10B cells and propagated in LB medium. The

MBP–Pas10p fusion protein was induced and then purified by affinity chromatography over amylose resin as described (Kalish *et al.*, 1995). Purified MBP–Pas10p, MBP–Pxr1p and MBP were analyzed by atomic absorption spectroscopy as described (Kalish *et al.*, 1995).

Antibodies, SDS–PAGE and Western blot analysis

Antibodies to Pas10p and yeast thiolase were generated by injecting bacterially synthesized proteins into rabbits. Crude anti-Pas10p and anti-thiolase sera were affinity purified as described (Crane *et al.*, 1994). Affinity-purified anti-Pas4p and anti-Pas7p antibodies are described elsewhere (Crane *et al.*, 1994; Kalish *et al.*, 1995). Secondary antibodies (horseradish peroxidase-conjugated goat anti-rabbit IgG antibodies) used for chemiluminescent detection of primary antibodies were obtained from Sigma. Proteins were separated by SDS–PAGE on either 4–15 or 4–20% gradient polyacrylamide gels (Bio-Rad) and analyzed by Western blot as described (Crane *et al.*, 1994). To reduce non-specific binding, Immobilon-P membranes (Millipore) were incubated with primary antibodies in a 10% non-fat dried milk (Carnation)/TBST solution (25 mM Tris–HCl, pH 7.4, 137 mM NaCl, 3 mM KCl, 0.1% Tween 20).

Subcellular fractionation, protease protection assays and enzyme assays

Differential centrifugation, subcellular fractionation, sodium carbonate extraction (Fujiki *et al.*, 1982a,b) and protease protection assays were performed as described (Crane *et al.*, 1994). For these experiments, equal amounts of each fraction (by proportion, not protein concentration) were analyzed by Western blot. Catalase activity was assayed as described by Peters *et al.* (1972), SDH was measured according to Pennington *et al.* (1961) and density was determined by refractometry.

Two-step flotation gradients

A 25 000 *g* pellet from *pas10*Δ cells was separated over a linear 32–60% sucrose gradient as described previously (Crane *et al.*, 1994). Fractions of 1 ml were collected from the bottom of the gradient and the refractive indices were measured. The five fractions with refractive indices that matched most closely with (i) the normal density catalase peak (fractions 11–15, Pop2) and (ii) the peroxisome membrane-rich peak (fractions 25–29, Pop1) were pooled. Aliquots of 200 µl from each pooled sample were transferred to a 5 ml Ultra-clear Beckman tube and overlaid with 2.4 ml 60% sucrose and then 2.4 ml 28% sucrose. The gradients were spun in a SW55 rotor at 170 000 *g* for 18 h at 4°C. Ten fractions of 0.5 ml were collected from the bottom of the gradients and each fraction was assayed for catalase activity, density and levels of Pas7p by Western blot analysis. Relative amounts of Pas7p were quantitated by densitometry.

Acknowledgements

We are most grateful to Michael Delannoy for his technical assistance with electron and confocal microscopy. We also thank Do Kim for affinity purifying the anti-Pas7p antibodies, Kasra Ramyar for assistance with PILE-UP analysis, Dr Jeremy Berg for suggestions regarding the zinc-binding studies and Dr Albert Mildvan for providing access to an atomic absorption spectrometer. This work was supported by a grant from the National Institutes of Health (DK45787) to S.J.G.

References

Aitchison,J.D., Murray,W.W. and Rachubinski,R. (1991) *J. Biol. Chem.*, **266**, 23197–23203.

Aitchison,J.D., Szilard,R.K., Nuttley,W.M. and Rachubinski,R.A. (1992) *Yeast*, **8**, 721–734.

Barlow,P.N., Luisi,B., Elliot,M. and Everett,R. (1994) *J. Mol. Biol.*, **237**, 201–211.

Berteaux-Lecellier,V., Picard,M., Thompson-Coffe,C., Zickler,D., Panvier-Adoutte,A. and Simonet,J. (1995) *Cell*, **81**, 1043–1051.

Blattner,J., Swinkels,B., Dörsam,H., Prospero,T., Subramani,S. and Clayton,D. (1992) *J. Cell Biol.*, **119**, 1129–1136.

Blattner,J., Dörsam,H. and Clayton,C.E. (1995) *FEBS Lett.*, **360**, 310–314.

Borden,K.L.B., Boddy,M.N., Lally,J., O'Reilly,J.O., Martin,S., Howe,K., Solomon,E. and Freemont,P.S. (1995) *EMBO J.*, **14**, 1532–1541.

Crane,D.I. and Gould,S.J. (1994) *Curr. Genet.*, **26**, 443–450.

Crane,D.I., Kalish,J.E. and Gould,S.J. (1994) *J. Biol. Chem.*, **269**, 21835–21844.

Cregg,J.M., Barringer,K.J., Hessler,A.Y. and Madden,K.R. (1985) *Mol. Cell. Biol.*, **5**, 3376–3385.

Cregg,J.M., Vankiel,I.J., Sulter,G.J., Veenhuis,M. and Harder,W. (1990) *Yeast*, **6**, 87–97.

Didion,T. and Roggenkamp,R. (1992) *FEBS Lett.*, **303**, 113–116.

Distel,B., Gould,S.J., Voorn-Brouwer,T., van der Berg,M., Tabak,H.F. and Subramani,S. (1992) *New Biologist*, **4**, 157–165.

Dodt,G., Braverman,N., Wong,C., Moser,A., Moser,H.W., Watkins,P., Valle,D. and Gould,S.J. (1995) *Nature Genet.*, **9**, 115–124.

Eitzen,G.A., Aitchison,J.D., Szilard,R.K., Veenhuis,M., Nuttley,M.W. and Rachubinski,R.A. (1995) *J. Biol. Chem.*, **270**, 1429–1436.

Elgersma,Y., van den Berg,M., Tabak,H.F. and Distel,B. (1993) *Genetics*, **135**, 731–740.

Erdmann,R., Veenhuis,D., Mertens,D. and Kunau,W.H. (1989) *Proc. Natl Acad. Sci. USA*, **86**, 5419–5423.

Erdmann,R., Wiebel,F.F., Flessau,A., Rytka,J., Beyer,A., Frohlich,K.U. and Kunau,W.H. (1991) *Cell*, **64**, 499–510.

Faber,K.N., Keizer-Gunnink,I., Pluim,D., Harder,W., Ab,G. and Veenhuis,M. (1995) *FEBS Lett.*, **357**, 115–120.

Freemont,P.S., Hanson,I.M. and Trowsdale,J. (1991) *Cell*, **64**, 483–484.

Fujiki,Y., Hubbard,A.L., Fowler,S. and Lazarow,P.B. (1982a) *J. Cell Biol.*, **93**, 97–102.

Fujiki,Y., Fowler,S., Shio,H., Hubbard,A.L. and Lazarow,P.B. (1982b) *J. Cell Biol.*, **93**, 103–110.

Gietl,C., Faber,K.N., van der Klei,I.J. and Veenhuis,M. (1994) *Proc. Natl Acad. Sci. USA*, **91**, 3151–3155.

Glover,J.R., Andrews,D., Subramani,S. and Rachubinski,R.A. (1994) *J. Biol. Chem.*, **269**, 7558–7563.

Gould,S.J., Keller,G.-A. and Subramani,S. (1987) *J. Cell Biol.*, **105**, 2923–2931.

Gould,S.J., Keller,G.-A. and Subramani,S. (1988) *J. Cell Biol.*, **107**, 897–905.

Gould,S.J., Keller,G.-A., Hosken,N., Wilkinson,J. and Subramani,S. (1989) *J. Cell Biol.*, **108**, 1657–1664.

Gould,S.J., Keller,G.-A., Schneider,M., Howell,S.H., Garrard,L.J., Goodman,J.M., Distel,B., Tabak,H. and Subramani,S. (1990a) *EMBO J.*, **9**, 85–90.

Gould,S.J., Krisans,S., Keller,G.-A. and Subramani,S. (1990b) *J. Cell Biol.*, **110**, 27–34.

Gould,S.J., McCollum,D., Spong,A.P., Heyman,J.A. and Subramani,S. (1992) *Yeast*, **8**, 613–628.

Gould,S.J., Kalish,J.E., Morrell,J.C., Bjorkman,J., Urquhart,A.J. and Crane,D.I. (1996) *J. Cell Biol.*, in press.

Grant,S.G., Jessee,J., Bloom,F.R and Hanahan,D. (1990) *Proc. Natl Acad. Sci. USA*, **87**, 4645–4649.

Hansen,H., Didion,T., Thiemann,A., Veenhuis,M. and Roggenkamp,R. (1992) *Mol. Gen. Genet.*, **235**, 269–278.

Helm,R., Cubitt,A.B. and Tsien,R.Y. (1995) *Nature*, **373**, 663–664.

Heyman,J.A., Mononsov,E. and Subramani,S. (1994) *J. Cell Biol.*, **127**, 1259–1273.

Hoffman,C.S. and Winston,F. (1987) *Gene*, **57**, 267–272.

Höhfeld,J., Veenhuis,M. and Kunau,W.H. (1991) *J. Cell Biol.*, **114**, 1167–1178.

Igual,J.C., Matallana,E., Gonzalez-Bosch,C., Franco,L. and Perez-Ortin,J.E. (1991) *Yeast*, **7**, 379–389.

James,G.L., Goldstein,J.L., Pathak,R.K., Anderson,R.G.W. and Brown,M.S. (1994) *J. Biol. Chem.*, **269**, 14182–14190.

Kalish,J.E., Theda,C., Morrell,J.C., Berg,J.M. and Gould,S.J. (1995) *Mol. Cell. Biol.*, **15**, 6406–6419.

Keller,G.-A., Gould,S.J., DeLuca,M. and Subramani,S. (1987) *Proc. Natl Acad. Sci. USA*, **84**, 3264–3268.

Keller,G., Krisans,S., Gould,S., Sommer,J., Schliebs,W., Kunau,W., Brody,S. and Subramani,S. (1991) *J. Cell Biol.*, **114**, 893–904.

Kunau,W.H., Beyer,A., Franken,T., Gotte,K., Marzioch,M., Saidowsky,J., Skaletz-Rorowski,A. and Wiebel,F.F. (1993) *Biochimie*, **75**, 209–224.

Lazarow,P.B. and Fujiki,Y. (1985) *Annu. Rev. Cell Biol.*, **1**, 489–530.

Lazarow,P.B. and Moser,H.W. (1995) In Scriver,C., Beaudet,A., Sly,W. and Valle,D. (eds), *Disorders of Peroxisome Biogenesis*. McGraw-Hill, New York, pp. 2287–2324.

Liu,H., Tan,X., Veenhuis,M., McCollum,D. and Cregg,J.M. (1992) *J. Bacteriol.*, **174**, 4943–4951.

Marzioch,M., Erdmann,R., Veenhuis,M. and Kunau,W.H. (1994) *EMBO J.*, **13**, 4908–4918.

McCammon,M.T., McNew,J.A., Willy,P.J. and Goodman,J.M. (1994) *J. Cell Biol.*, **124**, 915–925.

McCollum,D., Monosov,E. and Subramani,S. (1993) *J. Cell Biol.*, **121**, 761–774.

Miura,S., Kasuya-Arai,I., Mori,H., Miyazawa,S., Osumi,T., Hashimoto,T. and Fujiki,Y. (1992) *J. Biol. Chem.*, **267**, 14405–14411.
Motley,A., Hettema,E., Distel,B. and Tabak,H. (1994) *J. Cell Biol.*, **125**, 755–767.
Nuttley,W.M., Brade,A.M., Gaillardin,C., Eitzen,G.A., Glover,J.R., Aitchinson,J.D. and Rachubinski,R.A. (1993) *Yeast*, **9**, 507–517.
Osumi,T., Tsukamoto,T., Hata,S., Yokota,S., Miura,S., Fujiki,Y., Hijikata,M., Miyazawa,S. and Hashimoto,T. (1991) *Biochem. Biophys. Res. Commun.*, **181**, 947–954.
Pennington,R.J. (1961) *Biochem. J.*, **80**, 649–654.
Peters,T.J., Muller,M. and de Duve,C. (1972) *J. Exp. Med.*, **136**, 1117–1139.
Sambrook,J., Fritsch,E. and Maniatis,T. (1989) *Molecular Cloning: A Laboratory Manual*. Cold Spring Harbor Laboratory Press, Cold Spring Harbor, NY.
Sanger,F., Nicklin,S. and Coulson,A. (1977) *Proc. Natl Acad. Sci. USA*, **74**, 5463–5467.
Slawecki,M., Dodt,G., Steinberg,S., Moser,A.B., Moser,H.W. and Gould,S.J. (1995) *J. Cell Sci.*, **108**, 1817–1829.
Spong,A.P. and Subramani,S. (1993) *J. Cell Biol.*, **123**, 535–548.
Subramani,S. (1993) *Annu. Rev. Cell Biol.*, **9**, 445–478.
Swinkels,B.W., Gould,S.J., Bodnar,A.G., Rachubinski,R.A. and Subramani,S. (1991) *EMBO J.*, **10**, 3255–3262.
Swinkels,B.W., Gould,S.J. and Subramani,S. (1992) *FEBS Lett.*, **305**, 133–136.
Tan,X., Waterham,H.R., Veenhuis,M. and Cregg,J.M. (1995) *J. Cell Biol.*, **128**, 307–319.
Terlecky,S.R., Nuttley,W.M., McCollum,D., Sock,E. and Subramani,S. (1995) *EMBO J.*, **14**, 3627–3634.
Tolbert,N.E. (1981) *Annu. Rev. Biochem.*, **50**, 133–157.
Tsukamoto,T., Miura,S. and Fujiki,Y. (1991) *Nature*, **350**, 77–81.
van der Leij,I., Franse,M.M., Elgersma,Y., Distel,B. and Tabak,H.F. (1993) *Proc. Natl Acad. Sci. USA*, **90**, 11782–11786.
Voorn-Brouwer,T., Van der Leij,I., Hemrika,W., Distel,B. and Tabak,H.F. (1993) *Biochim. Biophys. Acta*, **1216**, 325–328.
Waterham,H.R., Titorenko,V.I., Swaving,G.J., Harder,W. and Veenhuis,M. (1993) *EMBO J.*, **12**, 4785–4794.
Waterham,H.R., de Vries,Y., Russell,K.A., Xie,W., Veenhuis,M. and Cregg,J.M. (1996) *Mol. Cell. Biol.*, **16**, 2527–2536.
Wiebel,F.F. and Kunau,W.-H. (1992) *Nature*, **359**, 73–76.
Yahraus,T., Braverman,N., Dodt,G., Kalish,J.E., Morrell,J.C., Moser, H.W., Valle,D. and Gould,S.J. (1996) *EMBO J.*, in press.
Zhang,J.W. and Lazarow,P.B. (1995) *J. Cell Biol.*, **129**, 65–80.

Received on January 2, 1996; revised on March 6, 1996